Vacancy-Assisted Halogen Reactions on Si(100)-(2 × 1)

Koji Nakayama,[1] C. M. Aldao,[2] and J. H. Weaver[1]
[1]*Department of Materials Science and Chemical Engineering, University of Minnesota, Minneapolis, Minnesota 55455*
[2]*Institute of Materials Science and Technology, Universidad Nacional de Mar del Plata-CONICET, Juan B. Justo 4302, 7600 Mar del Plata, Argentina*
(Received 20 July 1998)

Scanning tunneling microscopy studies of etching of Si(100)-(2 × 1) show that the rate of terrace pit formation goes through a maximum for surface coverages of $\theta(\mathrm{Cl}) = 0.77 \pm 0.05$ monolayer, in contrast to predictions of conventional models. Using recently calculated energies for different possible surface configurations, we show that a key component in desorption is the formation of a single-atom vacancy adjacent to a volatile $SiCl_2$ unit. The demonstration of vacancy-assisted reaction establishes a self-limited reaction and the sequence of events leading to desorption. [S0031-9007(98)08246-5]

PACS numbers: 61.16.Ch, 61.72.Ff, 81.65.–b

Etching refers to the removal of material from a surface by chemical means, and dry etching implies gas phase etchants and reactive products. Spontaneous dry etching is activated by thermal processes, and it can be assisted by photon, electron, or ion irradiation [1]. While etching is central to a wide range of technologies, including chip fabrication, the atomic sequences of events that occur are imprecisely known. Determining them challenges our ability to describe dynamic surface processes.

Descriptions of thermally activated etching have focused on what was naturally taken to be the central player, the desorbing molecule [2]. In the absence of a compelling reason to justify more complicated models, they treated the surface as a structurally stable backdrop that provided the heat reservoir needed for desorption. Here, we show that the Si(100) surface is not simply a structurally stable backdrop and that vacancy creation, in conjunction with $SiCl_2$ formation, is a key part of spontaneous etching with Cl. When single atom vacancies cannot be formed, because the surface is too rich in Cl, the etch rate drops precipitously. Thus, the etching agent itself reduces the reaction. Such self-limited inhibition is well known for heterogeneous catalysis where, assuming a Langmuir-Hinshelwood model, two reactants compete for active surface sites [3], but it was not expected for semiconductor etching reactions.

In this paper, we focus on thermally activated etching of Si(100)-(2 × 1) with Cl. With scanning tunneling microscopy (STM), we have determined the amount of Si removed as a function of the amount of Cl on the surface for a given set of processing conditions. For this surface, the terrace sites are initially equivalent, a single monovalent Cl atom reacts with each dangling bond of a dimer to form Si(100)-(2 × 1)-Cl, and temperature programmed desorption experiments [4–6] show there is only one important desorption product, $SiCl_2$. Conventional models would predict that the etch rate would increase monotonically with Cl concentration, $\theta(\mathrm{Cl})$. In contrast to expectations, we find a maximum when $\theta(\mathrm{Cl}) = 77 \pm 5\%$ and a sharp decrease as the surface became saturated.

The evolution of single-layer-deep pits during thermal etching of Si(100)-(2 × 1) has been investigated by Chander *et al.* [7] using STM. They reported that terrace pitting was initiated by dimer vacancy creation and that pit growth occurred preferentially along the dimer row direction, with occasional branching to neighboring rows. Motivated by the STM results, de Wijs, De Vita, and Selloni (WVS) [8] recently carried out first principles local density functional calculations of the energies of different Si-Cl configurations. They proposed a nonconventional model in which thermal creation of a single-atom vacancy adjacent to a $SiCl_2$ precursor enables its desorption. This paper explores the ramifications of the calculations, predicts coverage-dependent desorption rates, and establishes the connection to reaction rate reduction.

The experiments were performed in ultrahigh vacuum (base pressure 5×10^{-11} Torr) using an Omicron STM and RHK electronics. The preparation of clean Si(100)-(2 × 1) has been described elsewhere [7,9–11]. A solid-state electrochemical cell derived from AgCl doped with $CdCl_2$ was used to provide Cl_2 at a constant flux [7]. Procedurally, we dosed clean Si(100) to accumulate a given initial coverage, $\theta_i(\mathrm{Cl})$. To visualize the resulting adsorption structure and to directly quantify the concentration, we acquired dual bias STM images. In filled-state images, dimers with adsorbed Cl appeared darker than those that were Cl free because the density of states near E_F was decreased by Cl adsorption. The sample was then heated at a rate of $\sim 2.8\ \mathrm{K\,s^{-1}}$ to 800 K, held for 10 min, and quenched. This time-temperature regimen was chosen because it reduced the final Cl concentration, $\theta_f(\mathrm{Cl})$, to 50%–80% of $\theta_i(\mathrm{Cl})$. (Higher temperatures or extended annealing will ultimately desorb the Cl and allow the surface to recover from its etched state.) It was then imaged again to quantify $\theta_f(\mathrm{Cl})$ and the amount lost to desorption of $SiCl_2$. Finally, the amount of Si removed by etching could also be deduced by measuring the pit area in the images.

Figure 1 shows three STM images for samples having representative initial coverages. Each scanned area

 0031-9007/99/82(3)/568(4)$15.00

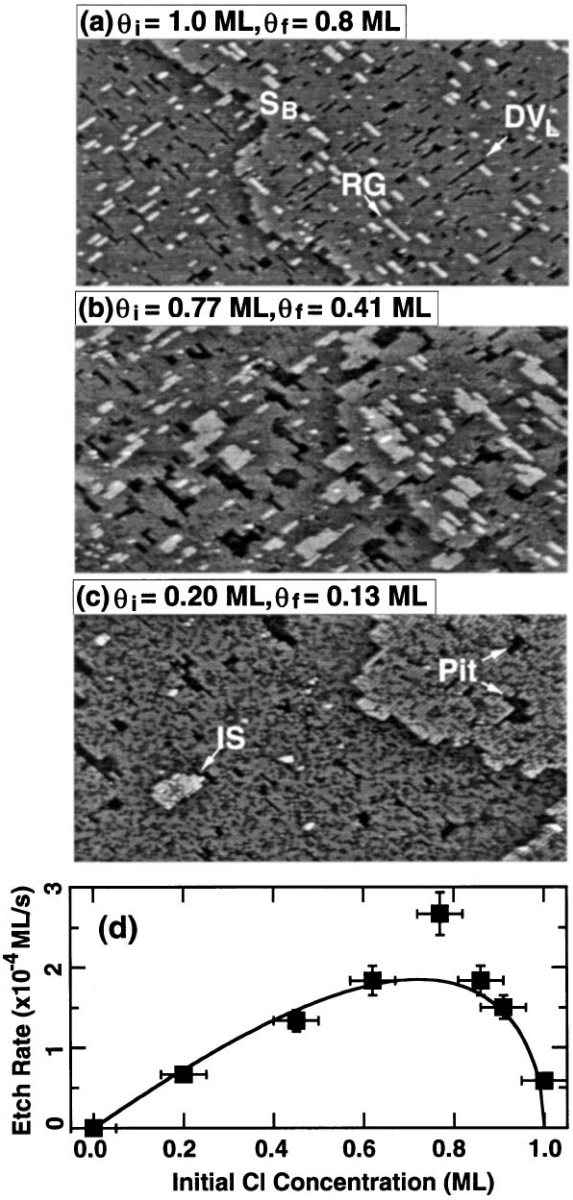

FIG. 1. STM images of Si(100)-(2 × 1) acquired at 300 K for dosed surfaces that were heated to 800 K for 10 min to activate etching. θ_i and θ_f are the initial and final concentration of Cl. An S_B step crosses each image, DV_L denotes a dimer vacancy line, and RG refers to regrowth features. 1000 × 500 Å^2; sample bias −2.5 V; current 0.2 nA. (a) High coverage etching is characterized by the elongation of dimer vacancy lines pits, the development of regrowth chains, and step retreat. (b) Intermediate coverage etching produces dimer vacancies, but these vacancies can also coalesce so that extended pits form by both etching and accretion. (c) Low coverage etching also results in extended pits, dark areas. (d) Data points representing the etching rate dc/dt vs θ_i(Cl) showing a maximum at 0.77 ± 0.05 ML. The solid line, obtained from Eq. (1), demonstrates reaction rate reduction.

includes an S_B-type step with the dimer row direction on the upper terrace being perpendicular to the step. Figure 1(a) shows the morphology achieved by etching when the Cl concentration was always high, $\theta_i(\mathrm{C1}) =$ 1 monolayer (ML) and $\theta_f(\mathrm{C1}) = 0.8$ ML. Pits that were initiated as single dimer vacancies grew along the dimer row direction, one dimer at a time, to produce vacancy lines, labeled DV_L. Vacancy diffusion in this regime was hindered by the high Cl concentration. Branching events expanded the pits, and some were two or three dimers in width [7]. Also apparent are bright chains that represent regrowth features, RG, built up from Si released from its terrace site when one Si atom of a dimer desorbs. These regrowth chains have formed against a Cl-rich surface. The results are similar to those observed after steady state etching with constant etchant flux [2,7,9,10]. Etching also roughened the steps and caused them to retreat.

Figure 1(b) was obtained for a surface with intermediate Cl concentration, $\theta_i(\mathrm{Cl}) = 0.77$ ML and $\theta_f(\mathrm{Cl}) =$ 0.41 ML. It shows large, single-layer-deep etch pits, regrowth features up to 7 rows in width, and a rougher S_B step profile. Differences compared to Fig. 1(a) demonstrate that dimer vacancies became more mobile as θ(Cl) decreased. Hence, pits could grow by accretion as vacancies coalesced or were captured. Etching at the perimeters of larger pits became more like step etching as they extended over many dimer chains. The step roughness was enhanced by the breakthrough of pits in the upper terrace and diffusion of vacancies to the step. Etching in this intermediate coverage regime gave surfaces with the greatest areal pit density.

Figure 1(c) shows the result of etching at low concentration, $\theta_i(\mathrm{Cl}) = 0.20$ ML and $\theta_f(\mathrm{Cl}) = 0.13$ ML. Because there was less Cl, the etch rate was considerably reduced and, when a vacancy was produced, it could diffuse easily. The extended dark areas correspond to pits that have grown by both accretion and etching. (In this image, the tip conditions were especially good and residual Cl could be identified as intermediate-gray dots. Chlorine concentrations were deduced from the images where atomic features could be resolved.) As for intermediate coverages, the regrowth islands are large. Step profiles were more regular because atom rearrangement at the steps was not impeded by Cl, the etch rate was slower, and there was little breakthrough with terrace pits.

To determine the amount of material removed as a function of the θ_i(Cl), we concentrated on large terraces with widths of ~500 Å. This minimized the possibility that Si atoms and vacancies could reach steps and be accommodated. The etch rate was the pit area divided by the time, 10 min. As summarized in Fig. 1(d), the overall etch rate increases with coverage until $\theta_i(\mathrm{Cl}) =$ 0.77 ± 0.05 ML. Thereafter, it decreases sharply. Indeed, the etch rate for a surface that was initially saturated was equal to that for $\theta_i(\mathrm{Cl}) = 0.20$ ML, namely, 5.8×10^{-5} ML/s.

To understand the downturn in Fig. 1(d), we must consider the possible reaction pathways and the energetics involved. To determine the relationship between the etch rate, dc/dt, and concentration θ(Cl), we assume that one step in the overall reaction is rate controlling and, from the activation energies [8], this must be the rate of

desorption of $SiCl_2$. All other steps are in equilibrium. Improvements to this model are indicated by the STM results, as discussed below.

The conventional etching pathway is depicted in Fig. 2(a). For any coverage, it starts with two monochlorinated Si atoms that constitute a surface dimer, $2SiCl(a)$. Isomerization produces a precursor molecule bound to the surface, $SiCl_2(a)$, as well as a Si atom having two dangling bonds, $Si(a)$. $Si(a)$ has generally been taken to be a "bystander" since it surrenders its Cl and remains on the surface when its more active partner desorbs. Thus, $2SiCl(a) \rightarrow SiCl_2(a) + Si(a) - E_1$, where E_1 is the energy of isomerization. Thermal desorption converts $SiCl_2(a)$ to gas phase $SiCl_2(g)$, and the no-longer-stabilized bystander moves onto the terrace to create a dimer vacancy, Fig. 2(a). Hence, $SiCl_2(a) + Si(a) \rightarrow SiCl_2(g) + Si(a) - E_2$, where E_2 is the activation energy of desorption. For this pathway, dc/dt should increase continuously with $\theta(\mathrm{Cl})$. From Fig. 1(d), this model fails to describe Si(100) etching.

WVS determined the energy barriers of Fig. 2(a), finding $E_1 = 1.4$ eV and $E_2 \sim 3.2$ eV at low coverage. From the reverse barrier, 0.7 eV, they concluded that $SiCl_2(a)$ would decay to $2SiCl(a)$ within $\sim$50 ns of its creation at 850 K. The calculated barrier, $\sim$4.6 eV, was much higher than experiment, 3–3.6 eV (Refs. [6] and [12]) and the etch rate would be negligible. Accordingly, they investigated alternate pathways and proposed the one shown in Fig. 2(b). The initial step was again the formation of $SiCl_2(a)$, but now the bystander was seen to escape onto the terrace before the reverse reaction could occur. The diffusion barrier of 0.6–1 eV can be easily overcome at 800 K [13]. Escape created a single vacancy next to $SiCl_2(a)$ at a cost of $E_3 = 0.03$ eV and eliminated the normal deexcitation pathway. Since the bystander would be unlikely for entropic reasons to return to the vacancy site, $SiCl_2(a)$ would have a much greater chance to desorb. WVS also considered that the new intermediate state could decay by transferring 2 Cl atoms to a dimer far away from the single vacancy, but the gain in doing so was only $E_4 = 0.05$ eV when the concentration was low.

To reveal the dependence of dc/dt on $\theta(\mathrm{Cl})$ for this model, we must consider the possible surface configurations, the relative energies that dictate the partitioning of Cl, and the desorption barriers for the precursor states. The seven relevant configurations depicted in Fig. 2(c) are [1] = a Si dimer, $Si_2(a)$; [2] = a dimer with one Cl, $Si_2Cl(a)$; [3] = a dimer with two Cl atoms, $2SiCl(a)$; [4] = a dimer with two Cl atoms and one bystander, $SiCl(a) + Si(a)$; [5] = same as [4] after the bystander escaped to create single vacancy, $SiCl_2(a)$ + SV; [6] = terrace dimer with the bystander that escaped, $Si_2(a) + Si(s)$; and [7] = unpaired Si atom of a dimer, $Si(a)$ + SV.

Etching occurs from [4], though at a negligible rate, and from [5], the new intermediate state. The bystander can escape onto the terrace at a cost of $E_3 = 0.03$ eV,

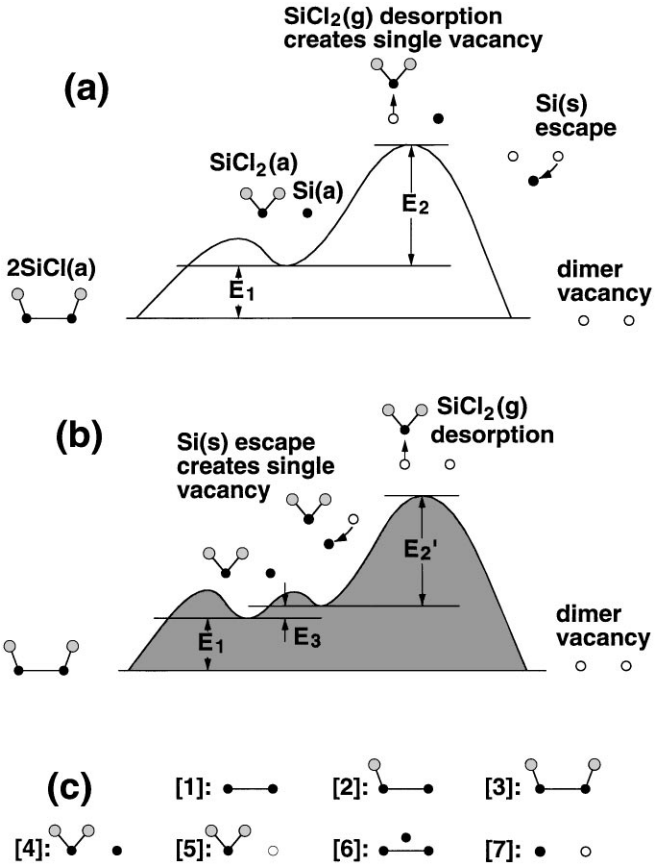

FIG. 2. (a) Conventional pathway for $SiCl_2$ desorption, starting from a dimer with two Cl atoms. Thermal activation produces the intermediate state and, ultimately, desorption. Thereafter, the "bystander" Si atom moves to the terrace and a dimer vacancy is formed. (b) Alternate pathway that shows vacancy formation from the intermediate state. This extends the lifetime of $SiCl_2(a)$ and increases the likelihood of desorption. (c) Representation of configurations [1]–[7] for Si and Cl on the surface, as discussed in the text.

$[1] + [4] \rightarrow [5] + [6] - E_3$, and here we require a Cl-free neighboring dimer that facilitates the escape. This requirement represents a key connection to $\theta(\mathrm{Cl})$ because Cl would block sites to which the bystander would move. This provides the needed mechanism that limits etching at high coverage.

There is a conservation equation for Si, $[1] + [2] + [3] + [4] + [5]/2 + 3[6]/2 + [7]/2 = 1$ which simplifies to $[1] + [3] = 1$ since these are the observable states for Si. For Cl, we have $[2]/2 + [3] + [4] + [5] = \theta(\mathrm{Cl})$ which reduces to $[3] = \theta(\mathrm{Cl})$ since pairwise occupancy is favored over single occupancy by $E_0 = 0.4$ eV per Cl pair [8]. Finally, Si adatoms must have been created on an ideal surface for dimer splitting, $[6] = [5] + [7]$. For simplicity, we assume dynamic equilibrium so that bystanders escape and return according to detail balance, since probabilities depend on the energies, 0.05 eV in this case. This underestimates the concentration of $SiCl_2(a)$ units adjacent to vacancies, [5], but it does not change the basic picture. An improved model would account

for coverage-dependent return by considering diffusion against a dynamic background of Cl, and it would include capture of bystanders to form regrowth structures, Figs. 1(a)–1(c).

In dynamic equilibrium, the concentrations of configurations differing by energies E_1, E_3, and E_4 are related by their Arrhenius dependence on temperature T. Thus, $[4]/[3] = \exp(-E_1/k_B T)$, where k_B is the Boltzmann constant. Similarly, $[5]\,[6]/[1]\,[4] = \exp(-E_3/k_B T)$, and $[3]\,[7]/[1]\,[5] = \exp(E_4/k_B T)$. Finally, the etching rate is proportional to the concentration of intermediate states, [5], which depends on $[3] = \theta(\mathrm{Cl})$. Accordingly,

$$dc/dt = b\{\exp[-(E_1 + E_3)/k_B T]\theta(\mathrm{Cl})[1 - \theta(\mathrm{Cl})]/\{1 + \exp(E_4/k_B T)[1 - \theta(\mathrm{Cl})]/\theta(\mathrm{Cl})\}\}^{1/2}, \quad (1)$$

where b is a proportionality constant. This provides a clear connection between vacancy-assisted etching and reaction self-limiting by an excess of Cl. In spite of its simplicity, the form for dc/dt is general since it does not depend strongly on the exact values of the parameters.

From Eq. (1), we obtained the solid line in Fig. 1(d), using $b = 18$. By treating the reduction in the reaction rate simply as site blocking, Eq. (1) predicts that the etch rate peaks at $\theta(\mathrm{Cl}) = 0.72$ ML. The only relevant parameter that would change the exact form dc/dt is E_4, the energy gained in transferring two Cl atoms from $SiCl_2$ far from the vacancy site, but there would be reaction inhibition and a turndown, independent of E_4. In deriving Eq. (1), we assumed that [1] and [3] are the dominant species, as shown by experiment [2,4–7,11].

In this Letter, we showed that STM results make it possible to assess the validity of reaction pathways [13]. They also point to improvements that would focus on the surface evolution during etching. While the calculations do not take into account the evolving surface structure, we see that the diffusivity of adatoms and vacancies, and therefore the surface structure, depends on coverage. As an isolated vacancy grows, as a dimer vacancy line evolves into an extended monolayer-deep pit, and as the regrowth islands change in shape, there must be corresponding changes in the population of the different desorption sites. We attribute any deviation from the simple form of Eq. (1) to these differences, and they are most profound near the peak etch rate, 0.77 ML. Second, Figs. 1(a) and 1(b) show that regrowth structures formed at high concentration are single dimers in width, but they are more extended at lower concentration. To properly describe the etching of regrowth features, it will be necessary to quantify Si atom diffusion against a background of Cl and to determine the desorption barriers and the Cl concentrations on regrowth features as a function of their size.

There are important implications that follow from these observations. First, increasing the flux in steady state etching can reduce rather than increase the etch rate. Second, etching at low temperature will be suppressed because of the high Cl concentration, an effect not considered before. Third, an increase in halogen concentration can inhibit the dominant pathway and increase the relative importance of pathways that are accessible only at high coverage. This last point can be seen from studies of Br-Si(100) where high coverage causes a unique 3×1 phase transformation and etching of atom rows rather than dimer rows [11].

We thank B. Y. Han, S. J. Chey, and L. Huang for useful discussion. This research was supported by the National Science Foundation and the Army Research Office.

[1] H. F. Winters and J. W. Coburn, Surf. Sci. Rep. **14**, 161 (1992), and references therein.

[2] For a detailed review, see J. H. Weaver and C. M. Aldao, "Spontaneous Halogen Etching of Si," in Morphological Organizations During Epitaxial Growth and Removal, edited by Z. Y. Zhang and M. G. Lagally (World Scientific, Singapore, to be published).

[3] C. G. Hill, Jr., *An Introduction to Chemical Engineering Kinetics and Reactor Design* (Wiley, New York, 1997), Chap. 6.

[4] Q. Gao, C. C. Cheng, P. J. Chen, W. J. Choyke, and J. T. Yates, Jr., J. Chem. Phys. **98**, 8308 (1993).

[5] N. Materer, R. S. Goodman, and S. R. Leone, J. Vac. Sci. Technol. A **15**, 2134 (1997).

[6] A. Szabo, P. D. Farrall, and T. Engel, Surf. Sci. **312**, 284 (1994).

[7] M. Chander, D. A. Goetsch, C. M. Aldao, and J. H. Weaver, Phys. Rev. Lett. **74**, 2014 (1995); Phys. Rev. B **52**, 8288 (1995).

[8] G. A. De Wijs, A. De Vita, and A. Selloni, Phys. Rev. Lett. **78**, 4877 (1997); Phys. Rev. B **57**, 10 021 (1998).

[9] M. Chander, Y. Z. Li, J. C. Patrin, and J. H. Weaver, Phys. Rev. B **RC47**, 13 035 (1993).

[10] D. Rioux, M. Chander, Y. Z. Li, and J. H. Weaver, Phys. Rev. B **49**, 11 071 (1994).

[11] K. Nakayama, C. M. Aldao, and J. H. Weaver, Phys. Rev. B (to be published).

[12] Q. Gao, Z. Dohnalek, C. C. Chey, W. J. Choyke, and J. T. Yates, Jr., Surf. Sci. **302**, 1 (1994).

[13] H. Feil, Phys. Rev. Lett. **74**, 1879 (1995). The energies used in Eq. (1) were obtained in 0 K calculations. Feil used molecular dynamics to examine the temperature dependence of the free energy barrier for desorption. He used the Stillinger-Weber potential and a model system derived from a 6 layer crystallite of Si with an adatom of Si placed on the 2×1 surface prior to saturation with Cl. The resulting surface moiety was taken to resemble $SiCl_3$ and the barrier for desorption was seen to decrease because of the number of configurations for $SiCl_3$ in the transition state. Equivalent calculations have not been reported for Si(100)-(2×1) where desorption involves the measured quantity, $SiCl_2$.